UV-Enhanced Room Temperature Ozone Sensor Based on Hierarchical SnO_2-In_2O_3

SUN Jian-bo[1], XU Jing[1], WANG Biao[2], SUN Peng[1], LIU Feng-min[1*] and LU Ge-yu[1]

1. State Key Laboratory on Integrated Optoelectronics, College of Electronic Science and Engineering, Jilin University, Changchun 130012, P. R. China;

2. Changchun Institute of Optics, Fine Mechanics and Physics, Chinese Academy of Sciences, Changchun 130033, P. R. China

Abstract SnO_2-In_2O_3 hierarchical microspheres were prepared by the hydrothermal and solvothermal method. The morphology, phase crystallinity of the obtained SnO_2-In_2O_3 were measured by X-ray diffraction(XRD), scan electron microscopy(SEM), respectively. A room temperature ozone sensor based on SnO_2-In_2O_3 hierarchical microspheres was fabricated and investigated. The gas sensing properties of the sensor using SnO_2-In_2O_3 strongly depended on the proportion of SnO_2 and In_2O_3. The sensitivity and response/recovery speed were greatly enhanced by UV illumination. A gas sensing mechanism related to oxygen defect was suggested.

Keywords Ozone sensor; Hierarchical SnO_2-In_2O_3; UV-Enhanced; Room temperature

Article ID 1005-9040(2012)-03-483-05

1 Introduction

Ozone is a strong oxidizing agent, widely used for purification, deodorization and sterilization in pharmaceutical, food, water supply and chemical industries[1—5]. However, it has deleterious effects on human health such as damaging the respiratory system[6]. Therefore, the measurement and monitor of ozone are very important. The measurement of ozone is typically carried out on analytical instruments based on photometric, chemiluminescence and fluorescence techniques, including iodide methods, passive sampling, mass spectrometry, and so on[7,8]. Though these analytical instruments are accurate and sensitive, they are large, expensive and complicated in operation, and not suitable for measuring the ozone in real-time. So, the development of small, low cost and high performance ozone sensor is urgently desired

With many advantages such as non-toxicity, economic raw material and reliable manufacturing process, gas sensors based on semiconducting metal oxides(MO) have received much attention in recent years. Some ozone sensors using MO(ZnO, In_2O_3, WO_3, MoO_3, TiO_2 and SnO_2) have been reported[9—15], whereas these sensors needed to be operated at high temperatures(over 150 °C) for accelerating the reaction of ozone on the surface of sensing materials and reducing the response/recovery time. In order to keep the ozone sensor to work at higher operating temperature, a heater is usually attached to the sensor, resulting in large power consumption.

In addition, the high operating temperature would speed up the growth of the MO particles and lead to the decreasing of long-term stability. UV illumination on semiconducting oxides can generate a great amount of photo-carriers and enhance the oxidation activity sites on the surface of MO. As a result, the operating temperature can be obviously decreased. Some studies about UV enhanced sensors for detecting ethanol, CO, H_2 and NO_2 have been reported[16—19]. Ozone sensor illuminated by UV light has been fabricated by Wang *et al.*[20]. However, the response speed needed to be further enhanced and accelerated for practical application. Francioso *et al.*[21] prepared SnO_2-In_2O_3 film and found that it possessed remarkable sensing property to oxidizing gases(NO_2 and O_3) at a lower temperature. However, the sensor based on SnO_2-In_2O_3 composites for detecting O_3 was rarely reported.

In the present work, the SnO_2-In_2O_3 hierarchical composites were prepared by hydrothermal and solvothermal method. For obtaining high sensing performance, the ratio of In_2O_3 to SnO_2 was optimized. The sensor based on the In_2O_3-SnO_2 hierarchical composite was fabricated and investigated.

2 Experimental

SnO_2-In_2O_3 hollow spheres were prepared by the following process. First, $SnCl_4 \cdot 5H_2O$(A. R. grade) and sucrose(A. R. grade) were completely dissolved in deionized water in 1:1 molar ratio. This solution was transferred to a teflon-lined stainless steel autoclave, which was then heated at 190 °C for 24 h. The resulting product was washed and dried, and then sintered at 450 °C for 2 h for gaining SnO_2 spherical shells. Second, $In(NO_3)_3 \cdot 5H_2O$ and *L*(+)-lysine monohydrate(99%, Acros Organics) as surfactant template(2:1, molar ratio) were added in the ethanol in sequence[22]. In order to coat In_2O_3 on the microsphere of SnO_2, the precursor was obtained by mixing SnO_2 spherical shell powder with the above solution in various

*Corresponding author. E-mail: liufm@jlu.edu.cn

Received December 19, 2011; accepted January 30, 2012.

Supported by the National Natural Science Foundation of China(Nos.60906036, 61074172, 61134010) and the Program for Changjiang Scholars and Innovative Research Team in Universities of China(No.IRT1017).

proportions[x=n(In):n(Sn), x=0.1, 0.125, 0.25, 1, 2, 4]. The obtained solution was transferred to a teflon-lined autoclave and solvothermally treated at 120 °C for 18 h. After cooling, the sample was washed five times with ethanol, then dried at 60 °C for 12 h in a vacuum drier. The product was sintered at 500 °C for 2 h, and the final product was named as IT0.1, IT0.125, IT0.25, IT1, IT2, IT4, according to proportions x=0.1, 0.125, 0.25, 1, 2 and 4, respectively.

The phase and crystallinity of the obtained samples were analyzed by X-ray diffraction(XRD, Rigaku D/MAX-2500V/PC, Cu $K\alpha$ line, λ=0.15418 nm). The morphologies of the obtained samples were observed by field-emission scanning electron microscopy(FESEM, JEOL JSM-7500F, Japan).

For fabricating the sensor, a paste was produced by mixing the obtained sample powder with deionized water and coated on the small alumina tube with two Au electrodes. After drying at room temperature for 1 h, the sensor element was sintered at 500 °C for 2 h. UV light-emitting diode(LED, operating power: 60 mW, luminous flux: 0.7 cd/m^2; peak wavelength: 380 nm) as light source was vertically placed over the sensor element.

The measurement system of gas sensing properties is shown in Fig.1. The sensor and UV LED were put in a sealed box[volume was 10 L; (10±1)% relative humidity(RH); 20 °C]. Ozone was prepared by an ozone generator(Ozonetec L-50B). The ozone generator can produce 90 μg of O_3 when it ran in an 10 L of air chamber for 5 min. Then a specified volume of various gases was injected into the box for producing a specified concentration of target gas. The resistance was measured with a multimeter(Fluke 8845A). The UV LED was driven with a power supply(Rigol 1380A). The response was defined as R_g/R_a, here, R_g and R_a are the resistances of the sensor in target gas and air, respectively.

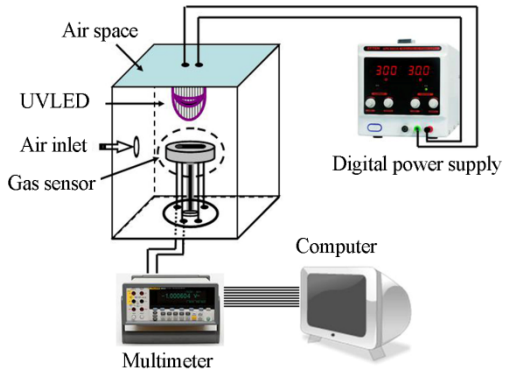

Fig.1 Measurement system of UV enhanced ozone sensor made from In_2O_3-SnO_2 hierarchical microspheres

3 Results and Discussion

3.1 XRD Analysis of Hollow Sphere SnO_2-In_2O_3

Fig.2 gives the XRD spectra of as-prepared samples. The diffraction peaks at 2θ=23.7°, 30.3°, 33.9° and 46.1° can be indexed to tetragonal rutile structure of SnO_2. With the In_2O_3 addition, the peaks at 2θ=19.2°, 27.5°, 31.7° and 40.8° indicating rhombohedral In_2O_3 increase gradually. The as-prepared powder is composed of SnO_2 and In_2O_3 and the other impurity can not be found. The calculated crystalline sizes of SnO_2 and In_2O_3 from Scherr equation are about 35 and 25 nm, respectively.

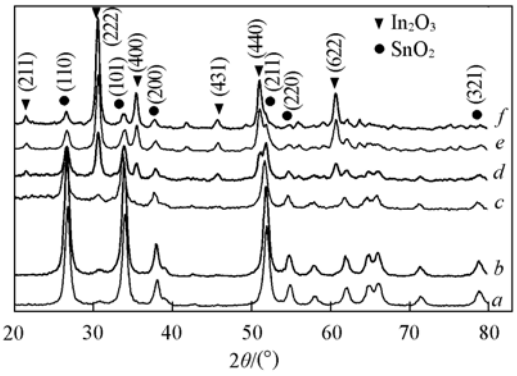

Fig.2 XRD patterns of hollow sphere SnO_2-In_2O_3 with various In:Sn molar ratios

a. IT0.1; *b*. IT0.125; *c*. IT0.25; *d*. IT1; *e*. IT2; *f*. IT4.

3.2 Morphology of Hollow Sphere SnO_2-In_2O_3

Surface topography and microstructures of various In_2O_3-SnO_2 composites were illuminated by FESEM. Panoramic FESEM images of as-sintered products are shown in Fig.3 with an enlarged image in the inset. With increasing the amount of In_2O_3, many slices composed of In_2O_3 nanoparticles staggered on the outside surface of spherical shell, and the spherical shell surface became much rougher.

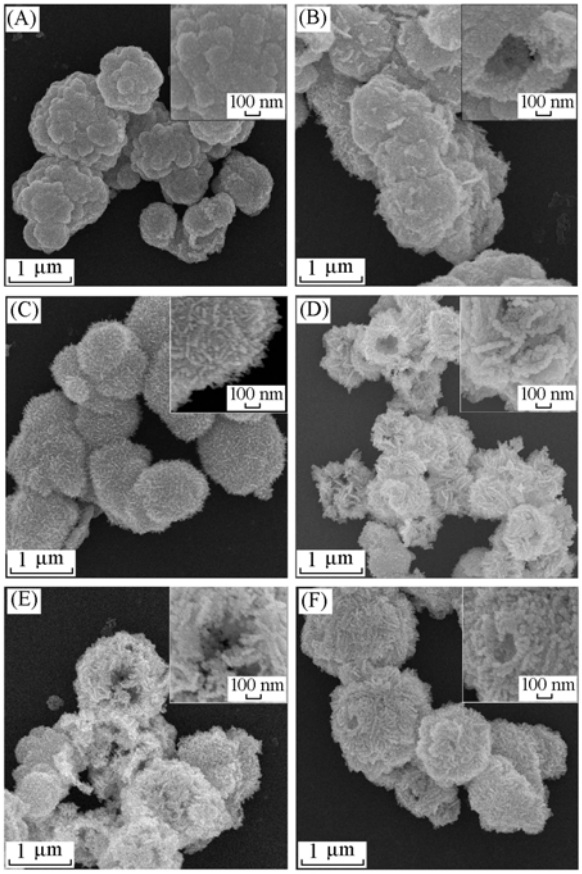

Fig.3 FESEM images of various In_2O_3-SnO_2 composites

(A) IT0.1; (B) IT0.125; (C) IT0.25; (D) IT1; (E) IT2; (F) IT4. Insets: enlarged images.

3.3 Possible Formation Mechanism of In_2O_3-SnO_2 Hierarchical Spheres

To reveal the growth process and possible growth mechanism of In_2O_3-SnO_2 hierarchical spheres, the study of the morphology evolution of hierarchical spheres with the change of reaction time(Fig.4) was conducted at 120 °C at a fixed precursor concentration. When the reaction was carried out for 1 h as shown in Fig.4(A), the sphere with rough surface was found, but InO(OH) particles could not be observed. When the reaction time reached to 3 h, the HS-SnO_2 sphere was covered by InO(OH) particles[Fig.4(B)]. It indicated that the model unit was composed of lysine and In^{3+} ions on the surface of the sphere. When the reaction time was further increased to 5 h [Fig.4(C)], InO(OH) nanosheets were formed on the surface of HS-SnO_2 sphere. With the reaction going on(10 h), the amount of InOOH nanosheets was increased, correspondingly, the diameter of the hollow sphere became large, as shown in Fig.4(D). When the reaction time reached to 18 h, the hollow sphere further grew, and the HS-SnO_2 was completely and uniformly coated by InO(OH) nanosheets[Fig.4(E)]. TEM image[Fig.4(F)] of the final product clearly shows that the SnO_2 hollow spheres were covered by InO(OH) nanosheets, which were composed of many nanoparticles[inset in Fig.4(F)].

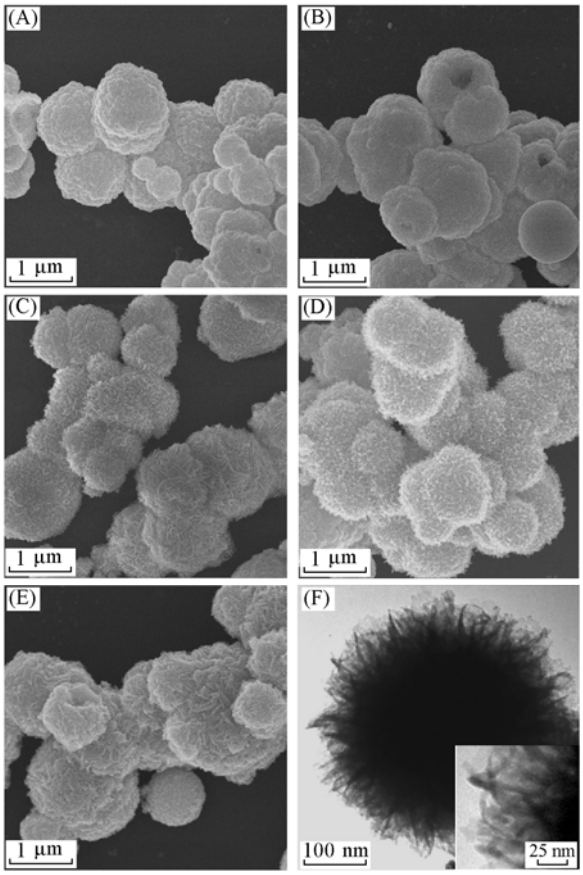

Fig.4 SEM(A—E) images of morphology evolution of In_2O_3-SnO_2 hierarchical nanostructures prepared at different reaction time and TEM image of hierarchical nanostructures(F)

(A) 1 h; (B) 3 h; (C) 5 h; (D) 10 h; (E) 18 h. (F) inset: enlarged image.

Based on the above results, a possible formation mechanism of In_2O_3-SnO_2 hierarchical spheres was proposed (Fig.5). Firstly, when $In(NO_3)_3$ and *L*(+)-lysine monohydrate(as anionic surfactant) were added in the solution, long-chain structures of indium with positive charge were formed due to indium ions(In^{3+}) bonding with a positive end of lysine. On the other hand, when the SnO_2 hollow spheres were introduced into the above solution, the surfactant could be adsorbed on the surface of SnO_2 spheres. Then the modifying layer with negative charges was formed on the surface of SnO_2 spheres(Fig.5 process *a*). Therefore, the long-chain structures of indium with positive charges would combine with the modifying layer with negative charges by Coulomb force, thus, an In^{3+} monolayer could be formed on the surface(Fig.5 process *b*). With the reaction progressing, InO(OH) nuclei would be formed and they grew on the surface of SnO_2 hollow spheres. Therefore, the surface of sphere was coated by a thin film of InO(OH) nanoparticles. In order to reduce the total surface free energy of a system, these nanoparticles would assemble into nanosheets[23,24](Fig.5 process *c*). Accordingly, hierarchical InO(OH)-SnO_2 spheres were formed in the solution. Finally, hierarchical In_2O_3-SnO_2 spheres were obtained by sintering at 500 °C for 2 h in air.

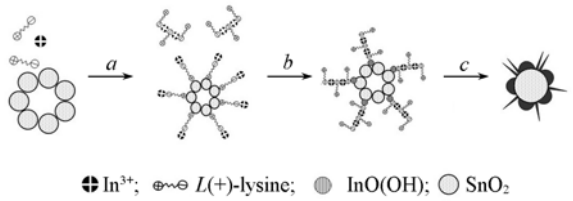

Fig.5 Formation mechanism of In_2O_3-SnO_2 hollow sphere

a. Absorbtion process; *b*. nucleation process; *c*. self-assembly growth process.

3.4 O_3 Sensing Characteristics

The sensing properties of sensors based on various In_2O_3-SnO_2 hollow spheres are shown in Fig.6. The sensor made from pure SnO_2 had no response to 1.8 μg/L ozone at room temperature both in dark and under UV light illumination. However, In_2O_3-SnO_2 hollow spheres displayed an obvious response to O_3. Among the prepared products, IT0.25 showed the largest response to O_3. When exposed to UV light, the sensor made from IT0.25 gave almost two times response greater

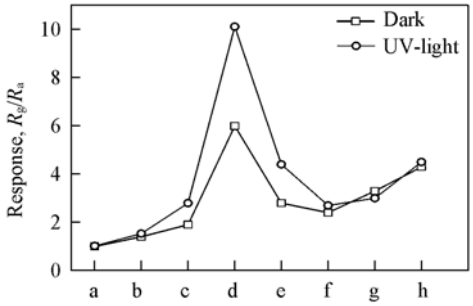

Fig.6 Dependence of response to 1.8 μg/L O_3 on molar ratio of In_2O_3 to SnO_2 at room temperature

Various devices: a. SnO_2; b. IT0.1; c. IT0.125; d. IT0.25; e. IT1; f. IT2; g. IT4; h. In_2O_3.

than that in dark. When molar ratio of In to Sn was small [n(In):n(Sn)<0.25:1], the response to O_3 increased with increasing the ratio, and arrived at a peak at n(In):n(Sn)=0.25. However, when the molar ratio of In to Sn became large [n(In):n(Sn)>0.25:1], In_2O_3 would partially cover the surface of SnO_2, and reduce the activated site on the surface of SnO_2 so that the response to O_3 decreased with the increasing of In_2O_3. When the molar ratio of In_2O_3 was further increased [n(In):n(Sn)>1:1], In_2O_3 would completely cover the surface of SnO_2 and played a leading role for the response of the sensor, as a result, the response to O_3 had a moderate increase with increasing the amount of In_2O_3.

Fig.7 gives the response and recovery transient of the sensor made from IT0.25 to 1.8 μg/L ozone with and without UV light illumination at room temperature. The response and recovery time were 90 and 350 s in the dark. With UV light illumination, the response and recovery time was shorten to 20 and 55 s. From Figs.6 and 7, it can be seen that under UV light illumination, the sensor using IT0.25 exhibited high sensitivity and fast response speed to O_3 even at room temperature.

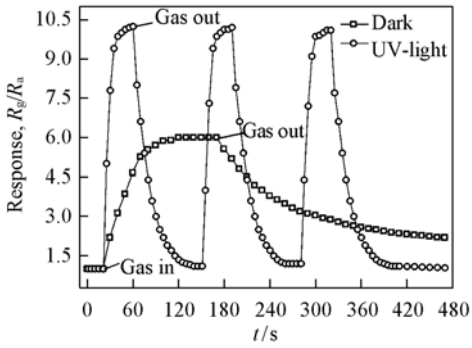

Fig.7 Response and recovery transient of the sensor made from IT0.25 to 1.8 μg/L ozone with and without UV light illumination at room temperature

The response of the sensor made from IT0.25 as a function of the O_3 concentration is presented in Fig.8. It is clear that the response of the sensor made from IT0.25 under UV light is larger than that in dark in the examined range of O_3 concentrations. In addition, the response of the sensor made from IT0.25 to a high concentration of O_3 didn't give the saturation trend opposite to the case in dark. Such an excellent sensing performance indicates that the sensor made from In_2O_3-SnO_2 hollow spheres has potential practical application.

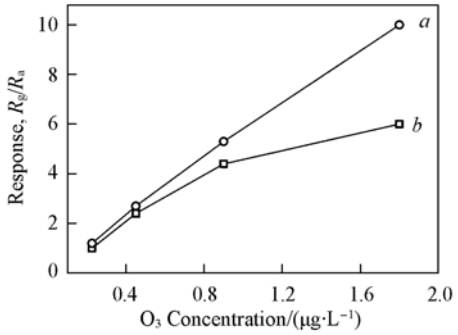

Fig.8 Relationship between the response of the sensor made from IT0.25 and the O_3 concentration with(*a*) and without(*b*) UV illumination at room temperature

3.5 Gas-sensing Mechanism

The resistance change of a semiconducting oxide type of gas sensor is based on the change of the carrier(electron or hole) concentration caused by the reaction of target gas on the surface of the semiconducting oxide. When the metal oxide acting as a sensing material is an n-type one, the resistance of the sensor decreases or increases in the reducing or oxidizing gases[25]. In_2O_3 and SnO_2 are typical n-type semiconducting oxides, the possible reactions of O_3 on the surface of theses metal oxides can be expressed as follow[26—28]:

$$O_3(gas) + e^- \longrightarrow O_3^-(ads) \quad (1)$$

$$O_3(gas) + e^- \longrightarrow O_2(gas) + O^-(ads) \quad (2)$$

Some investigations have revealed that the n-type conductivity of In_2O_3 or SnO_2 is caused by the oxygen lattice vacancies. Korotcenkov *et al*.[29] and Ivanovskaya *et al*.[30] investigated the delocalization of uncoupled electrons in In_2O_3 lattice with electronic spin resonance(ESR) spectroscopy and demonstrated that inherent defects of In_2O_3 are more than those of SnO_2. After combining In_2O_3 with SnO_2, more structural defects can be produced in the composite of In_2O_3 and SnO_2, which increases active surface state and is beneficial to the absorption of O_3.

When In_2O_3-SnO_2 microspheres were exposed to UV illumination, photo-generated carrier was produced, specially, electron concentration increases. Photo-generated carriers from In_2O_3 transfer to SnO_2 and participate in the reaction between the target gas and the surface of SnO_2, so the response increase[15,16]. Meanwhile, O_3 is activated by UV light, which benefits the rapid adsorption of it on the surface of sensing materials, and photocatalytic reduction reaction takes place so as to improve the response speed[31—33]. Similarly, UV light supplies adequate energy to desorption of O_3, thus reduces recovery time.

4 Conclusions

In_2O_3-SnO_2 hierarchical microspheres were prepared by hydrothermal and solvothermal method. When the molar ratio of In_2O_3 to SnO_2 is 1:4(IT0.25), the sensors based on these composites showed outstanding sensing properties to O_3 at room temperature with UV light. The response to 1.8 μg/L O_3 reached 10.12, response and recovery time was 20 and 55 s, respectively, under UV illumination.

References

[1] Marco S. L., Jos P., Gianluca L. P., *Sep. Purif. Technol*., **2010**, *72*, 235

[2] Wang L. P., Chun Y. X., Guo Y. Q., Chen Y. Z., Gao N. Y., *J. Env. Sci. Eng*., **2009**, *3*, 6

[3] Luigi D. N., Monica M., Federica S., Maria C. T., *J. Mater. Sci. Mater. Med*., **2010**, *21*, 2067

[4] Cullena P. J., Valdramidis V. P., Tiwari B. K., Patil S., Bourke P., *Ozone-Sci. Eng*., **2010**, *32*, 166

[5] Selin N. E., Wu S., Nam K. M., Reil J. M., Paltsev S., Mort G. P., *Environ. Res. Lett*., **2009**, *4*, 044014

[6] Hosoya Y., Itagaki Y., Aono H., Sadaoka Y., *Sens. Actuators B*, **2005**, *108*, 198
[7] Yasuko Y. M., Kunihiko A., Nakamura J., *Sens. Actuators B*, **2010**, *143*, 487
[8] Katsarakis N., Bender M., Cimalla V., Gagaoudakis E., Kiriakidis G., *Sens. Actuators B*, **2003**, *96*, 76
[9] Epifani M., Comini E., Arbiol J., Pellicer E., Siciliano P., Faglia G., Joan F., *J. Phys. Chem. C*, **2007**, *111*, 13967
[10] Korostynska O., Arshak K., Hickey G., Forde E., *Micro. Techno.*, **2008**, *14*, 557
[11] Korotcenkov G., Blinov I., Ivanova M., Stetter J. R., *Sens. Actuators B*, **2007**, *120*, 679
[12] Labidi A., Gaidi M., Guerin J., Bejaoui A., Maaref M., Aguir K., *Thin Solid Films*, **2009**, *518*, 355
[13] Galatsis K., Li Y. X., Wlodarski W., *Sens. Actuators B*, **2001**, *77*, 478
[14] Wu R. J.,Wu T. M., *Sens. Lett.*, **2010**, *8*, 564
[15] Mishra S., Ghanshyam C., Ram N., Bajapai R. P., Bedi R. K., *Sens. Actuators B*, **2004**, *97*, 387
[16] Sun J. B., Liu F. M., Zhong T. G., Xu J., Zhang Y. Q., Lu G. Y., *Sens. Lett.*, **2011**, *9*, 824
[17] Camagni P., Faglia G., Galinetto P., Perego C., *Sens. Actuators B*, **1996**, *31*, 99
[18] Fan S. W., Srivastava A. K., Dravid V. P., *Appl. Phys. Lett.*, **2009**, *95*, 142106
[19] Comini E., Faglia G., Sberveglieri G., *Sens. Actuators B*, **2001**, *78*, 73
[20] Wang C. Y., Cimalla V., Kups T., Rohling C. C., Stauden T., Ambacher O., *Appl. Phys. Lett.*, **2007**, *91*, 103509
[21] Francioso L., Forleo A., Capone S., Epifani M., Taurino A. M., Siciliano P., *Sens. Actuators B*, **2006**, *114*, 646
[22] Choi K. I., Kim H. R., Lee J. H., *Sens. Actuators B*, **2009**, *138*, 497
[23] Guo L., Yuan H. M., Huang K. K., Yuan L., Liu S. K., Feng S. H., *Chem. Res. Chinese Universities*, **2011**, *27*(5), 715
[24] Sun P., Zhao W., Cao Y., Guan Y., Sun Y. F., Lu G. Y., *CrystEngComm*, **2011**, *13*, 3718
[25] Maiti A., Rodriguez J. A., Law M., Kung P., McKinney J. R., Yang P. D., *Nano Lett.*, **2003**, *3*, 8
[26] Bulanin K. M., Lavalley J. C., Tsyganenko A. A., *J. Phys. Chem.*, **1995**, *99*, 10294
[27] Dhandapani B., Oyama S. T., *Appl. Catal. B: Environ*, **1997**, *11*, 129
[28] Pradesa J. D., Diaz R. J., Ramirez F. H., *Sens. Actuators B*, **2009**, *140*, 337
[29] Korotcenkov G., Cerneavschi A., Brinzari V., Vasiliev A., Ivanov M., Cornet A., Morante J., Cabot A., Arbiol J., *Sens. Actuators B*, **2004**, *99*, 297
[30] Ivanovskaya M., Bogdanov P., Faglia G., Sberveglieri G., *Sens. Actuators B*, **2000**, *68*, 344
[31] Xirouchaki C., Kiriakidis G., Pedersen T. F., *J. Appl. Phys.*, **1996**, *12*, 9349
[32] Masato T., Norifumi H., Isao T., *Electr. Comm.*, **2005**, *7*, 1423
[33] Ecke G., Wang C. Y., Cimalla V., Ambacher O., *Phys. Stat. Sol.*, **2008**, *6*, 1603